Supporting Information

Synthesis and Lewis Acid Properties of a Ferrocene-Based Planar-Chiral Borenium Cation

Jiawei Chen, Roger A. Lalancette and Frieder Jäkle*

Department of Chemistry, Rutgers University-Newark, 73 Warren Street, Newark, NJ, USA. Fax: +1 973 353 1264; Tel: +1 973 353 5064; E-mail: fjaekle@rutgers.edu

1. Reagents and General Methods

$PhBCl_2$ and Et_3PO were purchased from Aldrich and used without further purification. (p*S*)-**1**,[1] Mosher's acid,[2] and the Krossing salts[3] were prepared according to literature procedures. All reactions and manipulations were carried out under an atmosphere of prepurified nitrogen using either Schlenk techniques or an inert-atmosphere glove box (MBraun). 499.9 MHz ^{1}H NMR, 125.7 MHz ^{13}C NMR, 160.4 MHz ^{11}B NMR, and 470.4 MHz ^{19}F spectra were recorded on a Varian INOVA NMR spectrometer (Varian Inc., Palo Alto, CA) equipped with a boron-free 5 mm dual broadband gradient probe (Nalorac, Varian Inc., Martinez, CA). Solution ^{1}H and ^{13}C NMR spectra were referenced internally to solvent signals. ^{11}B NMR spectra were acquired with boron-free quartz NMR tubes and referenced to $BF_3 \cdot Et_2O$ ($\delta = 0$). The following abbreviations are used for signal assignments: Lu = 3,5-dimethylpyrid-2yl, Fc = ferrocenyl, Cp = cyclopentadienyl. High resolution MALDI-MS data (benzo[α]pyrene as matrix) were obtained in positive mode on an Apex Ultra 7.0 Hybrid FTMS (Bruker Daltonics). UV/Vis absorption data were acquired on a Varian Cary 500 UV/Vis/NIR spectrophotometer. Optical rotation analyses were performed on an Autopol III polarimeter, Rudolph Research Analytical, using a tungsten-halogen light source operating at λ = 589 nm. GC-FID analyses were performed on a Varian CP3800 GC instrument using an Rt-BetaDex-sm chiral column. Chiral HPLC analyses were performed on a Waters Empower system equipped with a 717plus autosampler, a 1525 binary HPLC pump, and a 2998 photodiode array detector; a CHIRALPAK® IA-3 column was used for separation. Elemental analyses were performed by Quantitative Technologies Inc., Whitehouse, NJ.

X-ray diffraction intensities were collected on a Bruker SMART APEX CCD Diffractometer using CuKα (1.54178 Å) radiation at 100 K. The structures were refined by full-matrix least squares based on F^2 with all reflections (SHELXTL V5.10; G. Sheldrick, Siemens XRD, Madison, WI). Non-hydrogen atoms were refined with anisotropic displacement coefficients, and hydrogen atoms were treated as idealized contribution. SADABS (Sheldrick, 12 G.M. SADABS (2.01), Bruker/Siemens Area Detector Absorption Correction Program; Bruker AXS: Madison, WI, 1998) absorption correction was applied. Crystallographic data for the structures of (p*R*)-**3**$^+$ and (p*R*)-**3**$^+$**(acetophenone)** have been deposited with the Cambridge Crystallographic Data

Center as supplementary publications CCDC 907178-907179. Copies of the data can be obtained free of charge on application to CCDC, 12 Union Road, Cambridge CB2 1EZ, UK (fax: (+44) 1223-336-033; email: deposit@ccdc.cam.ac.uk).

2. Synthetic Procedures and Characterization Details

Synthesis of [(p*R*)-LuFcB(C_6H_5)Cl · 0.5 C_7H_8] ((p*R*)-2). A solution of (p*S*)-**1** (100 mg, 0.22 mmol) in a mixture of hexanes/toluene (10/10 mL) was cooled down to –37 °C and then a solution of $PhBCl_2$ (70 mg, 0.44 mmol, 2.0 equiv) in toluene (2 mL) was added dropwise under stirring. The mixture was stirred over night at room temperature before applying high vacuum to remove the solvents. The residue was taken back up in a mixture of hot hexanes/toluene (1/1). When stored at –37 °C crystals were obtained that contain half an equivalent of toluene. Yield: 55 mg (55%). $[\alpha]^{20}_D$ (c = 0.10, CH_2Cl_2) = 2110°. ^{1}H NMR (499.9 MHz, $CDCl_3$, 25 °C): Major : Minor = 2.5 : 1; δ = 8.23 (s, 1H, Lu; Minor), 8.13 (s, 1H; Lu, Major), 7.58 (s, 1H; Lu, Minor), 7.53 (d, *J* = 7 Hz, 2H; *o*-Ph, Minor), 7.48 (s, 1H; Lu, Major), 7.37 (pst, *J* = 7 Hz, 2H; *m*-Ph, Minor), 7.32 (d, *J* = 7 Hz, 2H; *o*-Ph, Major), 7.26 (nr, 1H, p-Ph, Minor), 7.16 (pst, *J* = 7 Hz, 2H; *m*-Ph, Major), 7.13 (m, 1H, *p*-Ph, Major), 4.77 (dd, J = 2.5 Hz, 1.0 Hz, 1H; Cp, Major), 4.71 (overlapped, 2H; Cp, Minor), 4.62 (dd, J = 2.5 Hz, 1.0 Hz, 1 H; Cp, Major), 4.58 (m, 2H; Cp, Major + Minor), 4.22 (s, 5H; free Cp, Major), 3.65 (s, 5H; free Cp, Minor), 2.52 (s, 3H; Lu-Me, Major), 2.51 (s, 3H; Lu-Me, Minor), 2.38 (s, 3H; Lu-Me, Minor), 2.30 (s, 3H; Lu-Me, Major). ^{11}B NMR (160.4 MHz, $CDCl_3$, 25° C) δ = 6.0 ($w_{1/2}$ = 210 Hz). ^{13}C NMR (125.69 MHz, $CDCl_3$, 25 °C) δ = 158.3, 157.3, 143.3, 142.8, 142.4, 141.5, 131.5, 131.5, 130.4, 130.3, 129.5, 128.9, 127.3, 127.3, 126.4, 126.2 (Lu + Ph), ipso-Ph-B not observed, 84.0 (ipso-Cp-C, Major), 82.5 (ipso-Cp-C, Minor), 74.7 (Cp, Minor), 74.4 (Cp, Major), 70.3 (ipso-Cp-B, Major), 70.2 (ipso-Cp-B, Minor), 70.1 (free Cp, Major), 69.8 (free Cp, Minor), 64.6 (Cp, Minor), 64.5 (Cp, Major), 18.3 (Lu-Me, Major), 18.3 (Lu-Me, Minor), 18.2 (Lu-Me, Minor), 18.1 (Lu-Me, Major). UV-Vis (CH_2Cl_2): λ_{max} = 413 (ε = 1900 M^{-1} cm^{-1}), 503 (ε = 2700 M^{-1} cm^{-1}). High-resolution MALDI-MS (+ mode, benzo[α]pyrene): m/z 413.0828 ($[M]^+$, 40%, calcd for $^{12}C_{23}{}^1H_{21}{}^{11}B^{14}N^{35}Cl^{56}Fe$ 413.0804); m/z 378.1137 ($[M\text{-}Cl]^+$, 100%, calcd for $^{12}C_{23}{}^1H_{21}{}^{11}B^{14}N^{56}Fe$ 378.1115).

Synthesis of [(p*R*)-LuFcB(C_6H_5)]$^+${Al[OC(CF_3)$_3$]$_4$}$^-$ ((p*R*)-3$^+$). Method A: To a solution of LuFcB(C_6H_5)Cl · 0.5 C_7H_8 ((p*R*)-**2**; 4.9 mg, 0.0106 mmol) in $CHCl_3$ (0.5 mL) that was cooled down to –37 °C was added a solution of [Ag(CH_2Cl_2)]{Al[OC(CF_3)$_3$]$_4$} (14.0 mg, 0.012 mmol, 1.1 equiv) in $CHCl_3$ (0.5 mL) under stirring. The color of the solution turned from red to purple. After filtering off a small amount of a white precipitate, the filtrate was carefully layered with 1 mL of hexanes and kept at –37 °C for recrystallization. Yield: 6.0 mg (42 %). **Method B:** To a sample of Li{Al[OC(CF_3)$_3$]$_4$} (13.4 mg, 0.0138 mmol) in a 10 mL Schlenk flask was added a solution of LuFcB(C_6H_5)Cl · 0.5 C_7H_8 ((p*R*)-**2**; 6.3 mg, 0.0138 mmol) in $CDCl_3$ (1 mL) under vigorous stirring. Upon addition the color of the solution turned from red to purple. The mixture was stirred for 2 hours and then filtered. ^{1}H NMR analysis showed complete conversion to the product. ^{1}H NMR (499.9 MHz, $CDCl_3$, 25 °C): δ = 8.31 (s, 1H; Lu), 7.95 (d, *J* = 7 Hz, 2H; *o*-

Ph), 7.83 (s, 1H; Lu), 7.81 (nr, 1H; *p*-Ph), 7.67 (pst, *J* = 7 Hz, 2H; *m*-Ph), 5.75 (nr, 1H; Cp), 5.58 (nr, 1H; Cp), 5.48 (nr, 1H; Cp), 4.32 (s, 5H; free Cp), 2.40 (s, 3H; Lu-Me), 2.39 (s, 3H; Lu-Me). ^{13}C NMR (125.69 MHz, $CDCl_3$, 25 °C): δ = 156.4, 148.0, 140.1, 134.6, 134.5, 134.1, 131.6, 129.9, (Lu + Ph), 121.2 (q, *J*(C,F) = 293 Hz, CF_3), 85.7 (Cp), 82.9 (ipso-Cp-C), ipso-Cp-B not observed, 79.2 (Cp), 76.6 (Cp), 76.5 (free Cp), 17.7 (Lu-Me), 17.2 (Lu-Me). ^{11}B NMR (160.4 MHz, $CDCl_3$, 25 °C) δ = 45.4 ($w_{1/2}$ = 750 Hz). ^{19}F NMR (470.4 MHz, $CDCl_3$, 25 °C): δ = –75.4. UV-Vis (CH_2Cl_2): λ_{max} = 407 (ε = 2000 M^{-1} cm^{-1}), 566 (ε = 2200 M^{-1} cm^{-1}). Elemental analysis for $C_{39}H_{21}AlBF_{36}FeNO_4$, calcd C 34.82, H 1.57, N 1.04, found C 34.32, H 1.27, N 0.96%.

Synthesis of [(p*R*)-LuFcB(C_6H_5)·PhC(O)CH_3]$^+${Al[OC(CF_3)$_3$]$_4$}$^-$ ((p*R*)-3$^+$(acetophenone)). In a glove box, a solution of LuFcB(C_6H_5)Cl · 0.5 C_7H_8 ((p*R*)-**2**; 11.0 mg, 0.0242 mmol) in CH_2Cl_2 (5 mL) was added to a sample of Li{Al[OC(CF_3)$_3$]$_4$} (23.5 mg, 0.0242 mmol) in a vial under vigorous stirring. Upon addition the color of the solution turned from red to purple. The mixture was stirred for 2 hours and then a solution of PhC(O)CH_3 in CH_2Cl_2 (1.0 M, 0.0242 mmol, 0.0242 mL) was added. The color of the solution turned from purple to red. The solution was filtered and concentrated under high vacuum. The residue was re-dissolved in CH_2Cl_2 (5 mL), carefully layered with hexanes (5 mL) and then placed in a freezer at –37 °C to obtain purple red crystals. Yield: 20 mg (57 %). ^{1}H NMR (499.9 MHz, CD_2Cl_2, 25 °C): δ = 8.31, 8.03, 7.76, 7.37 (br, 10H; Ph), 8.22 (s, 1H; Lu), 7.76 (s, 1H; Lu), 5.16 (br, 1H; Cp), 5.02 (br, 1H; Cp), 4.72 (br, 1H; Cp), 4.02 (s, 5H; free Cp), 3.15 (br, 3H; Me), 2.54 (s, 3H; Lu-Me), 2.42 (s, 3H; Lu-Me). ^{1}H NMR (499.9 MHz, CD_2Cl_2, –20 °C): δ = 8.43 (d, *J* = 8 Hz, 2H; *o*-Ph), 8.17 (s, 1H; Lu), 8.11 (t, *J* = 8 Hz, 1H; *p*-Ph), 7.82 (t, *J* = 8 Hz, 2H; *m*-Ph), 7.72 (s, 1H; Lu), 7.32-7.26 (m, 3H; *m*-Ph + *p*-Ph), 7.22 (d, *J* = 7 Hz, 2H; *o*-Ph), 5.09 (nr, 1H; Cp), 4.90 (nr, 1H; Cp), 4.60 (nr, 1H; Cp), 3.94 (s, 5H; free Cp), 3.26 (s, 3H; Me), 2.53 (s, 3H; Lu-Me), 2.39 (s, 3H; Lu-Me). ^{11}B NMR (160.4 MHz, $CDCl_3$, 25 °C) δ = 10.7 ($w_{1/2}$ = 960 Hz). Elemental analysis for $C_{47}H_{29}AlBF_{36}FeNO_5$, calcd C 38.52, H 1.99, N 0.96, found C 38.36, H 2.04, N 0.95%.

Hydrosilylation Catalysis. Stock solutions (1.0 M) of the ketones and silanes were prepared in CH_2Cl_2. A predetermined quantity of (*p*R)-**3**$^+$ was dissolved in a minimum amount of CH_2Cl_2 and the corresponding amount of the silane solution was added. The mixture was cooled down to –37 °C, an equimolar amount of the ketone solution was added and the progress of the reaction was monitored by taking an aliquot and measuring the ^{1}H NMR in CD_2Cl_2. After completion of the reaction, the mixture was treated with dilute HCl (aq.) solution and stirred vigorously overnight. To determine the enantioselectivity, the resulting (desilylated) alcohol was either directly examined by chiral GC-FID or HPLC, or isolated by distillation and then reacted with the chemical shift reagent (S)-(+)-α-methoxy-α-trifluoromethylphenylacetyl chloride as described by Mosher[2]. In a typical procedure, to a solution of the alcohol (5 mg) in 0.7 mL of $CDCl_3$ in a NMR tube is added 1 equivalent of Mosher's chemical shift reagent and an excess amount of pyridine-d5. The mixture is heated to 50 °C for 2 days and then filtered. The filtrate is transferred to another NMR tube and measured directly.

References

(1) Chen, J.; Lalancette, R. A.; Jäkle, F. *Organometallics* **2013**, *to be submitted*.
(2) Dale, J. A.; Mosher, H. S. *J. Am. Chem. Soc.* **1973**, *95*, 512.
(3) a) Krossing, I. *Chem. - Eur. J.* **2001**, *7*, 490. b) Reisinger, A.; Trapp, N.; Krossing, I. *Organometallics* **2007**, *26*, 2096.

Table S1. Hydrosilylation of different ketones with silanes in the presence of (*p*R)-**3**$^+$ as catalyst.

Entry	Ketone	Silane	Cat. (%)	Conv. (%)[a]	ee (%)	
1	R^1=Ph, R^2=Me	Et_3SiH	5	65	20[b]	R-(+)
2	R^1=Ph, R^2=Me	$PhMe_2SiH$	5	92	6[b]	R-(+)
3	R^1=Ph, R^2=Me	Ph_3SiH	5	trace	ND	
4	R^1=*t*Bu, R^2=Me	Et_3SiH	2	>95	5[c]	S-(+)
5	R^1=*t*Bu, R^2=Me	$PhMe_2SiH$	2	>95	5[c]	S-(+)
6	R^1=1-Np, R^2=Me	Et_3SiH	3	29	ND	
7	R^1=1-Np, R^2=Me	$PhMe_2SiH$	3	44	ND	

[a] Conversion determined by ^{1}H NMR (reaction time: ca. 12 h except for entries 4,5 which went to completion within 10 min).

[b] The silylated product was first converted to the corresponded alcohol, then the ee was determined by chiral GC-FID (Entry 1) or HPLC (Entry 2).

[c] The silylated product was converted to the corresponded alcohol, isolated by distillation, and then reacted with the chemical shift reagent (S)-(+)-α-methoxy-α-trifluoromethylphenylacetyl chloride as described by Mosher (*J. Am. Chem. Soc.* **1973**, *95*, 512-519)

(a) Data corresponding to Entry 1 in Table S1 – Chiral GC-FID analysis of 1-phenylethanol:

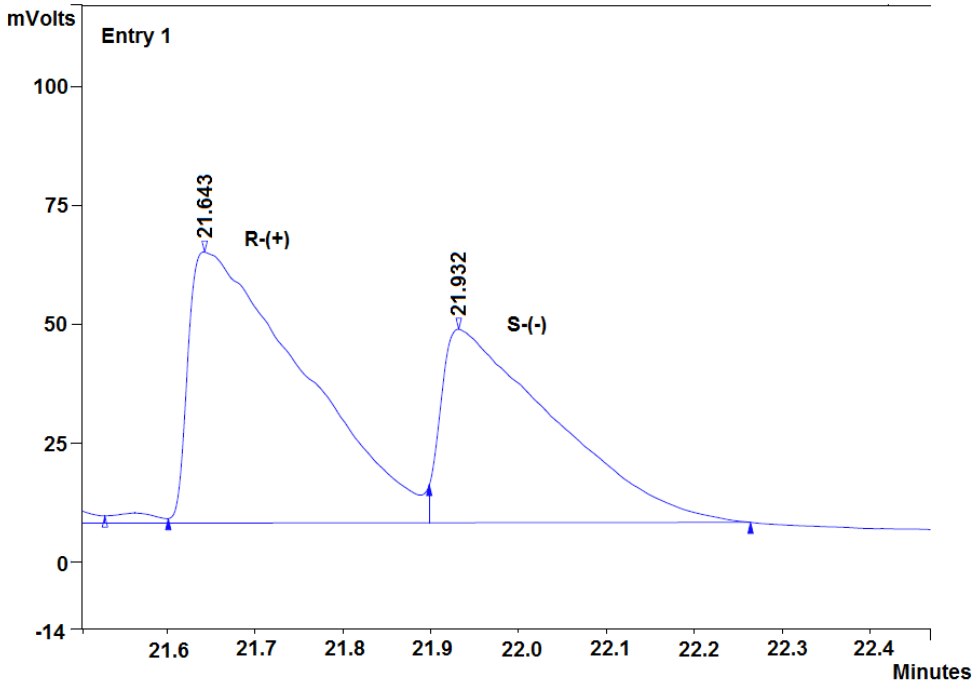

(b) Data corresponding to Entry 2 in Table S1 – Chiral HPLC analysis of 1-phenylethanol:

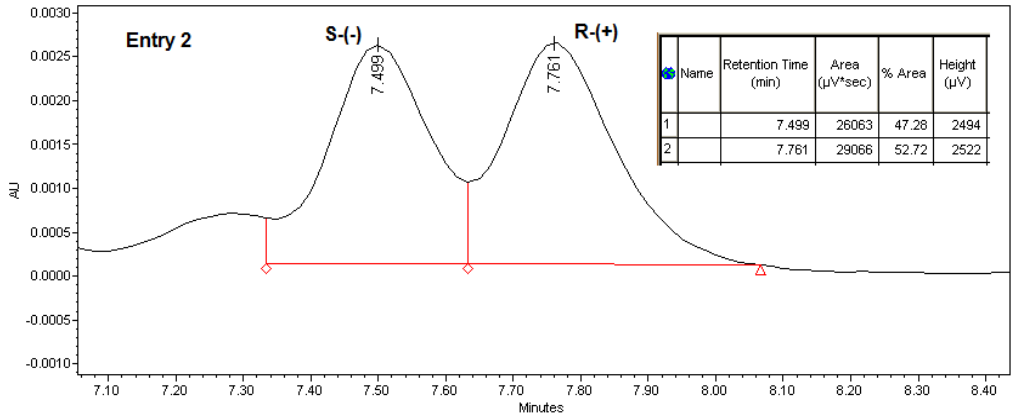

(c) Data corresponding to Entry 4 in Table S1 – ^{1}H NMR spectrum of the product from reaction of 3,3-dimethyl-2-butanol with Mosher's chemical shift reagent:

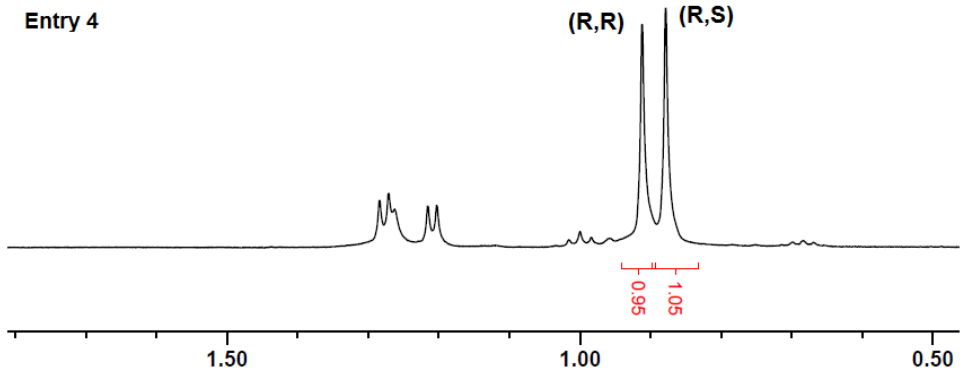

(d) Data corresponding to Entry 5 in Table S1 – ^{1}H NMR spectrum of the product from reaction of 3,3-dimethyl-2-butanol with Mosher's chemical shift reagent:

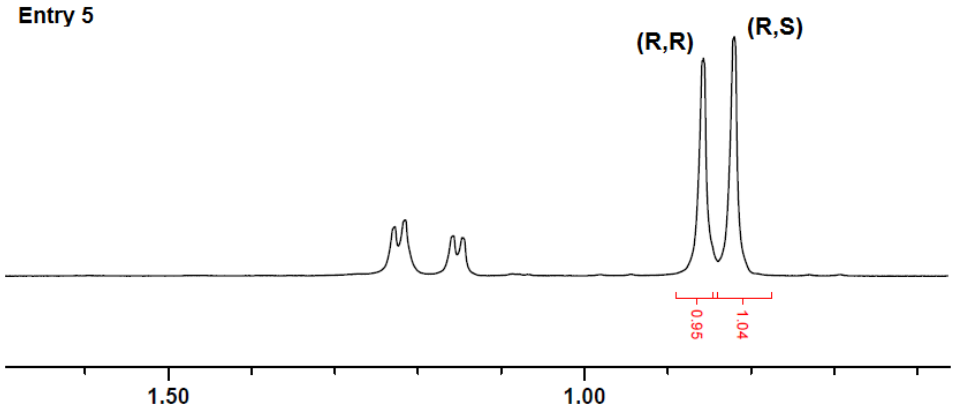

(d)

Figure S1. Data corresponding to determination of enantiomeric excess of catalysis products

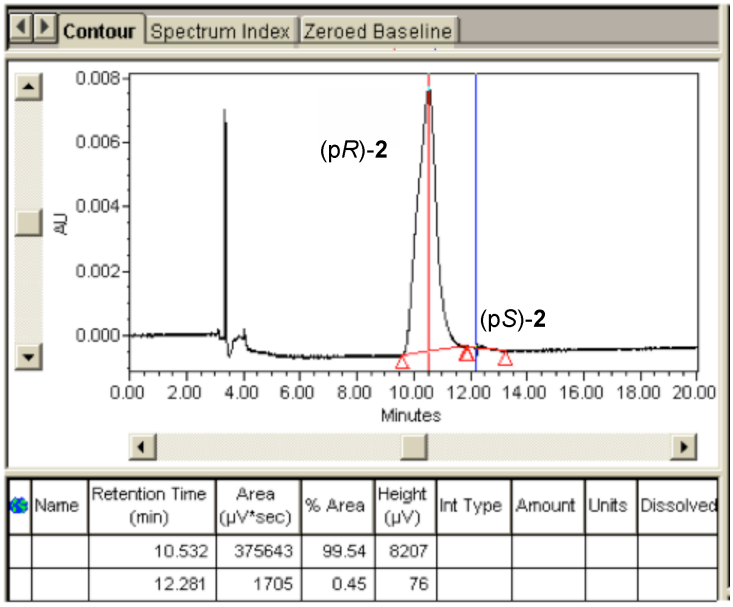

Name	Retention Time (min)	Area (µV*sec)	% Area	Height (µV)	Int Type	Amount	Units	Dissolved
	10.532	375643	99.54	8207				
	12.281	1705	0.45	76				

Figure S2. Chiral HPLC analysis for compound (*p*R)-**2** (99% ee) in 93:7 hexanes:THF.

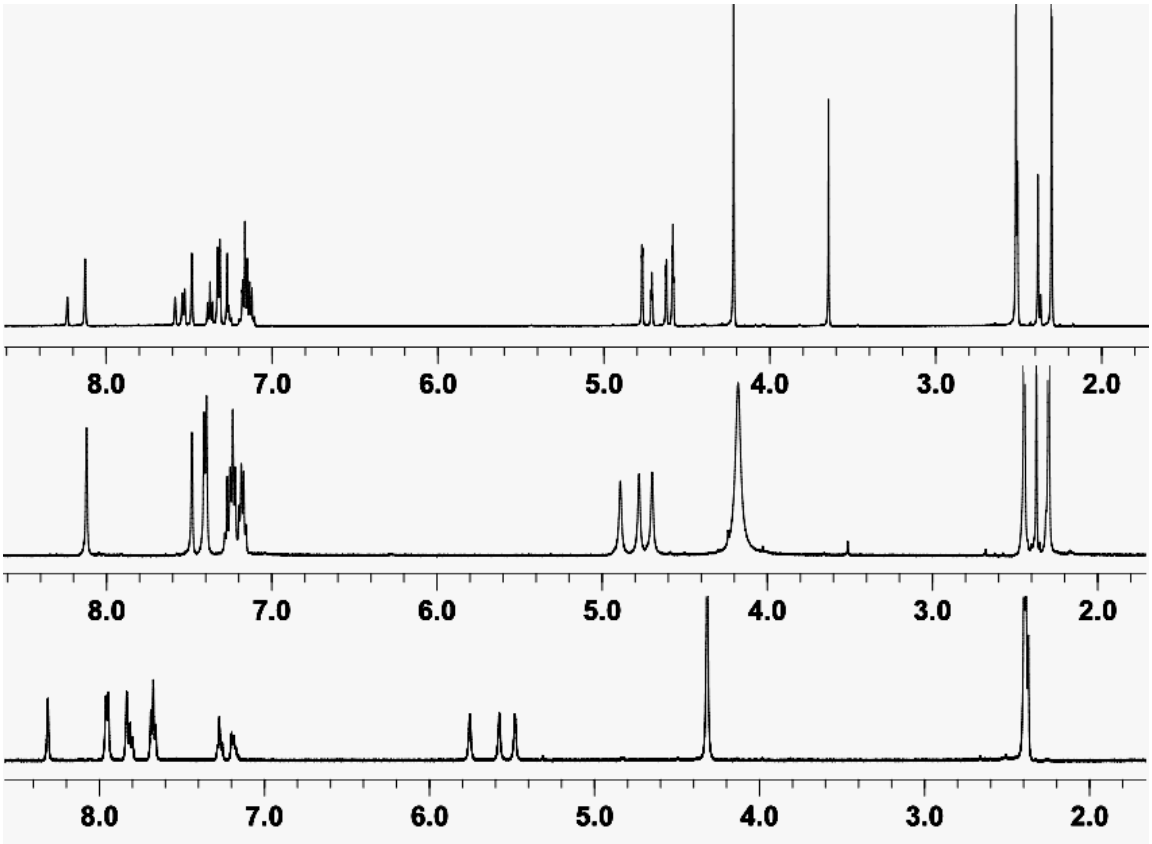

Figure S3. Complete ^{1}H NMR spectra of (p*R*)-**2** (top), (p*R*)-**2** + $B(C_6F_5)_3$ (middle), and (p*R*)-**3**$^{+}$ (bottom) in $CDCl_3$.

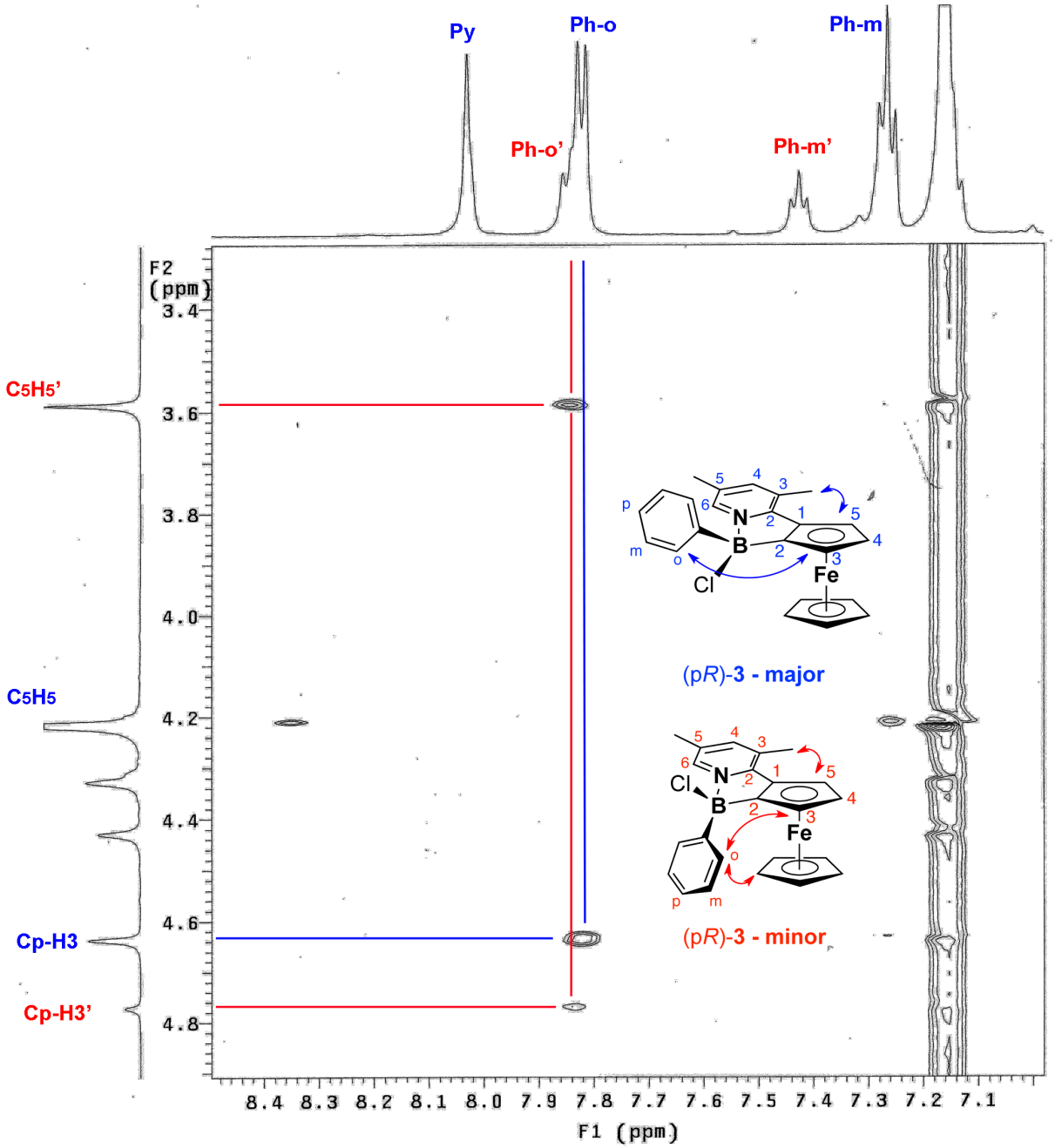

Figure S4. 2D-NOESY spectra of compound (p*R*)-**2** in C_6D_6.

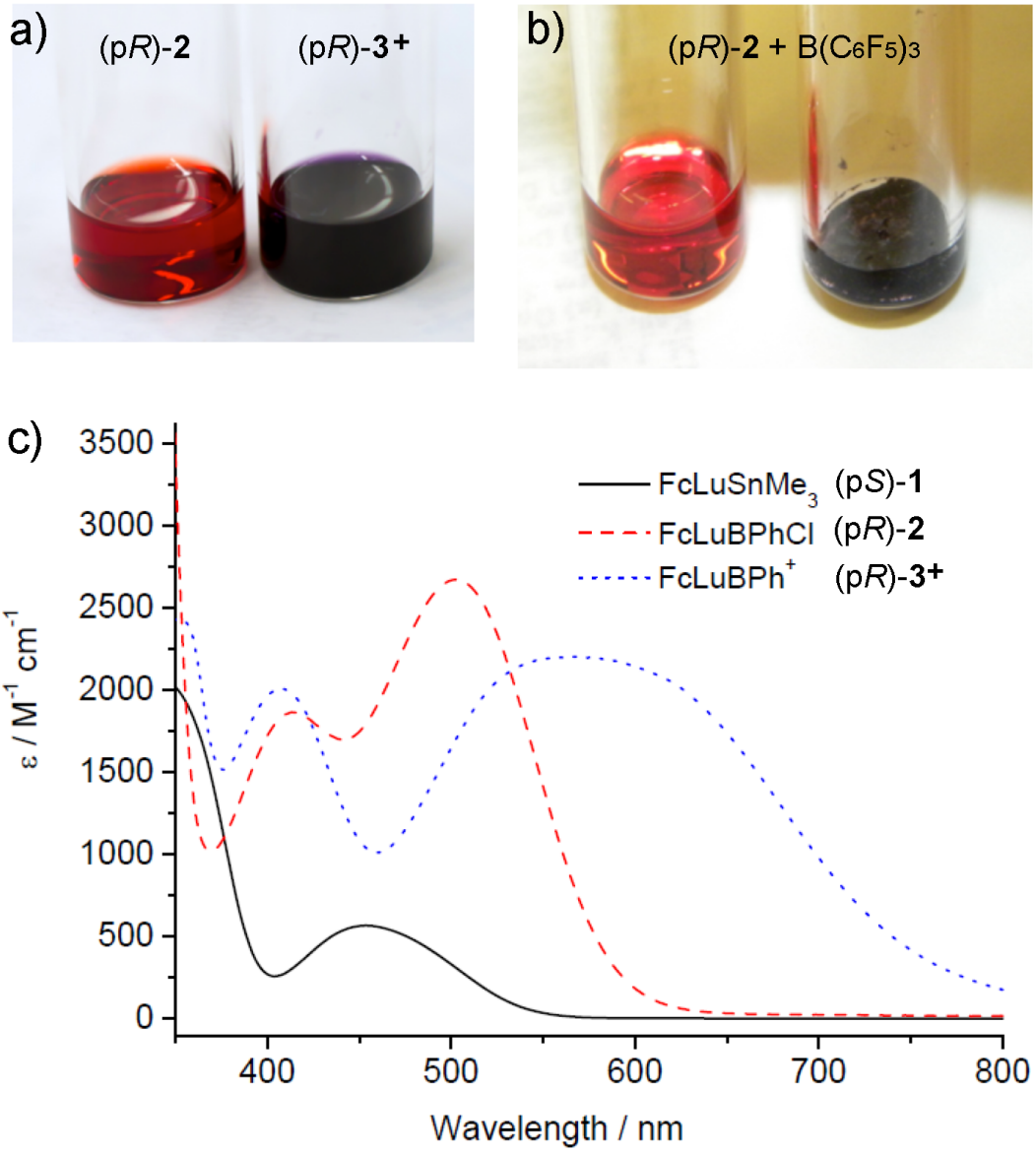

Figure S5. a) Photographs of CH_2Cl_2 solutions of compounds (p*R*)-**2** and (p*R*)-**3**$^+$. b) Photographs of a mixture of (p*R*)-**2** + $B(C_6F_5)_3$ in CH_2Cl_2 solution and in the solid state after solvent removal. c) Comparison of UV-Vis spectra of compounds (p*S*)-**1** ($CHCl_3$), (p*R*)-**2** and (p*R*)-**3**$^+$ (CH_2Cl_2).

Note that the color change upon removal of solvent from the mixture of (p*R*)-**2** + $B(C_6F_5)_3$ in CH_2Cl_2 suggests that halide abstraction by $B(C_6F_5)_3$ with formation of (p*R*)-**3**$^+$ becomes more favorable in the absence of the solvent CH_2Cl_2.

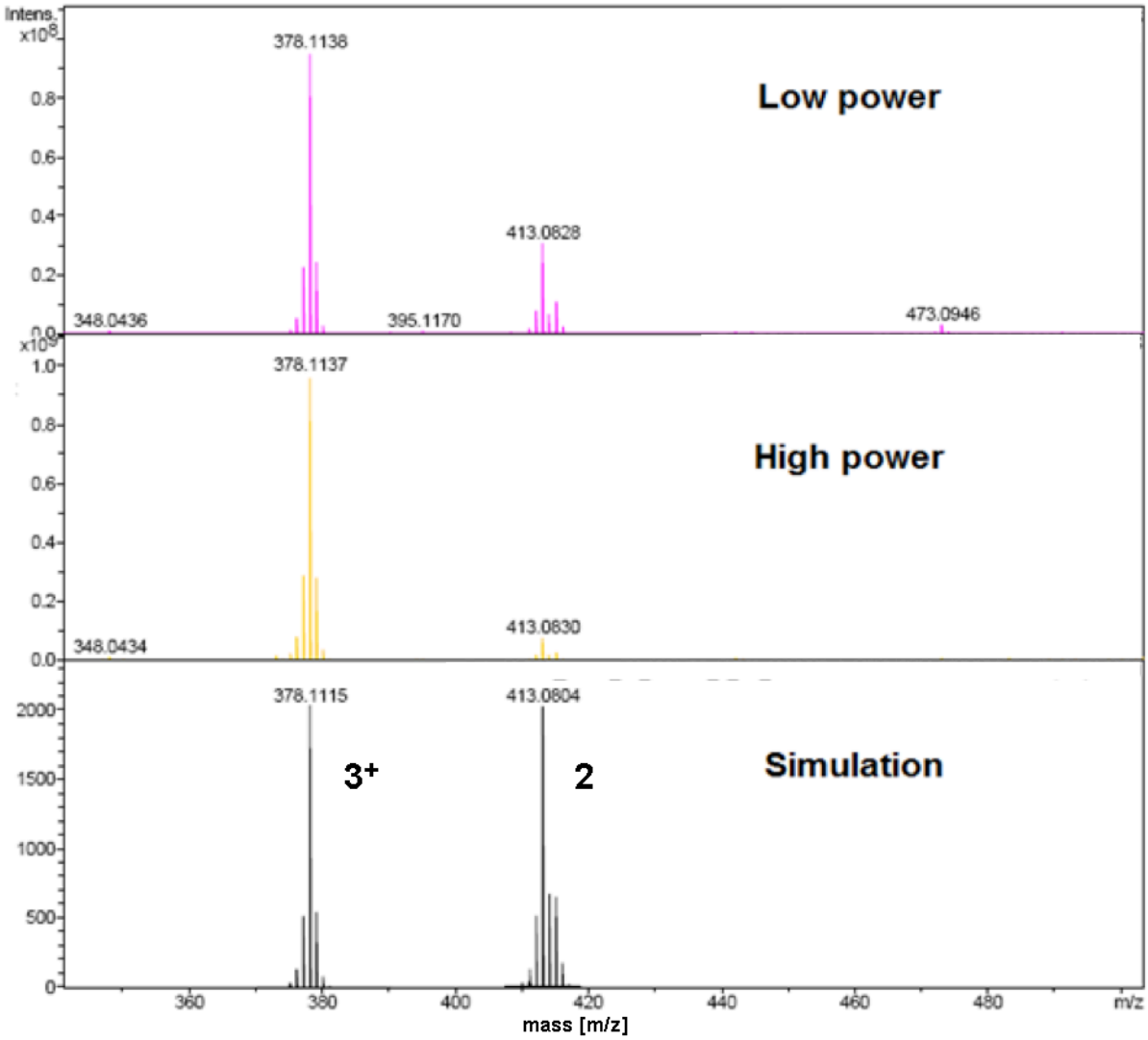

Figure S6. High-resolution MALDI-MS spectra of compound (p*R*)-**2** acquired at different laser power levels and comparison to simulated spectra of (p*R*)-**2** and (p*R*)-$\mathbf{3}^{+}$. With increasing laser power, the ion (p*R*)-$\mathbf{3}^{+}$ becomes more dominant, suggesting facile Cl^{-} abstraction under these conditions.

Lewis Acidity Determination

The Gutman-Becket method (Beckett, M. A.; Brassington, D. S.; Coles, S. J.; Hursthouse, M. B. *Inorg. Chem. Commun.* **2000**, *3*, 530.) was utilized to examine the relative Lewis acidity of (p*R*)-**3**$^+$. The chemical shift difference Δδ is larger for (p*R*)-**3**$^+$ (32.6 ppm) than for $B(C_6F_5)_3$ (26.5 ppm), which would indicate higher Lewis acidity of (p*R*)-**3**$^+$ toward Et_3PO. However, in a competition experiment (d), more of the adduct $Et_3PO{\bullet}B(C_6F_5)_3$ than of $Et_3PO){\bullet}$(p*R*)-**3** is generated. This shows that $B(C_6F_5)_3$ is a stronger Lewis acid toward Et_3PO. The fact that the ^{31}P chemical shift difference is larger for the binding of Et_3PO to (p*R*)-**3**$^+$ could be related to delocalization of the positive charge on the phosphorous. Clearly, the Gutmann-Becket method cannot be used to directly compare the Lewis acidity of ionic and neutral borane species, instead a competition experiment has to be performed.

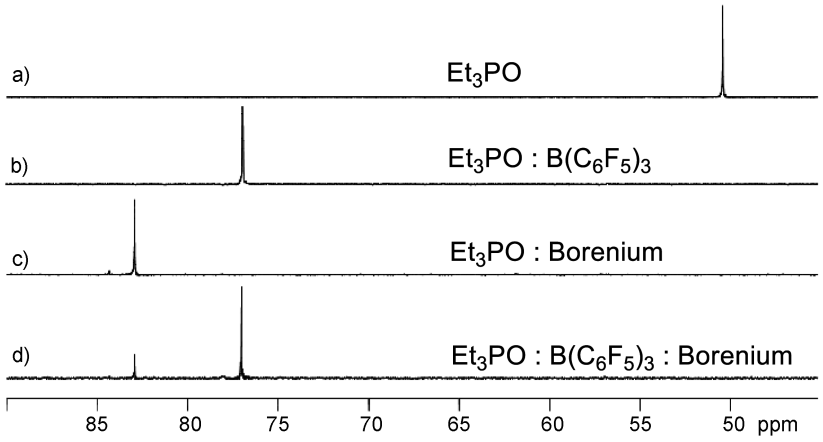

	δ (^{31}P) [/ppm]
Et_3PO	50.4
$Et_3PO{\cdot}B(C_6F_5)_3$	76.9
Δδ for $B(C_6F_5)_3$	**26.5**
$Et_3PO{\cdot}$(p*R*)-**3**$^+$	83.0
Δδ for (p*R*)-3$^+$	**32.6**

Figure S7. Competitive binding of (p*R*)-**3**$^+$ and $B(C_6F_5)_3$ to Et_3PO examined by ^{31}P NMR spectroscopy in CD_2Cl_2 at room temperature (0.02 M solutions). a) Et_3PO; b) Et_3PO + $B(C_6F_5)_3$. c) Et_3PO + (p*R*)-**3**$^+$. d) 1 Et_3PO + 1 (p*R*)-**3**$^+$ + 1 $B(C_6F_5)_3$.

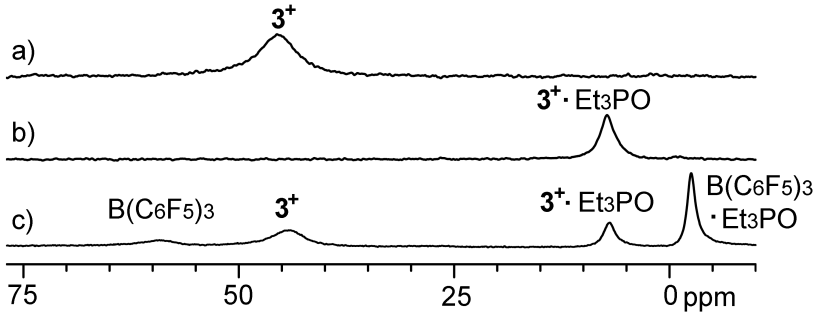

Figure S8. Competitive binding of (p*R*)-**3**$^+$ and $B(C_6F_5)_3$ to Et_3PO examined by ^{11}B NMR spectroscopy in CD_2Cl_2 at room temperature (0.02 M solutions). a) (p*R*)-**3**$^+$; b) (p*R*)-**3**$^+$ + Et_3PO; c) 1 (p*R*)-**3**$^+$ + 1 $B(C_6F_5)_3$ + 1 Et_3PO. The ratios in plot c) are consistent with those obtained by ^{31}P NMR (see Figure S7).

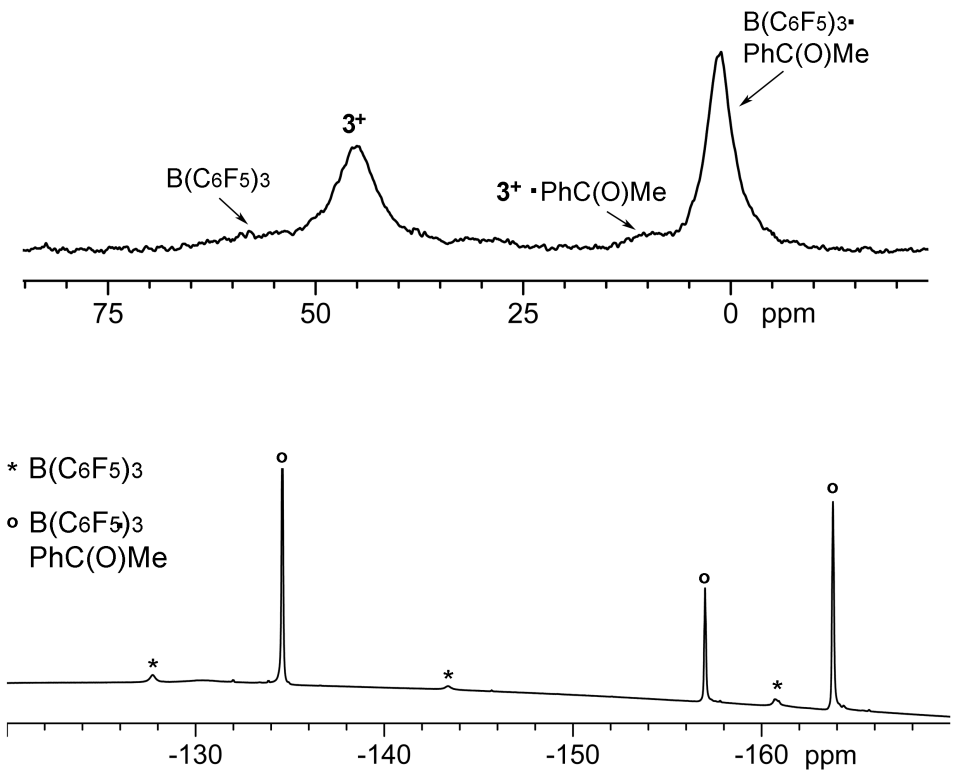

Figure S9. (top) Competitive binding of (p*R*)-**3**$^+$ and $B(C_6F_5)_3$ to acetophenone (ratio of (p*R*)-**3**$^+$: $B(C_6F_5)_3$: PhC(O)Me) = 1 : 1 : 1) examined by ^{11}B NMR spectroscopy in CD_2Cl_2 at –20 ºC. (bottom) Corresponding ^{19}F NMR data. The ratio of the complexation products was estimated to be ca. 10:1 in favor of complex formation with $B(C_6F_5)_3$, which is significantly larger than in the case of Et_3PO.

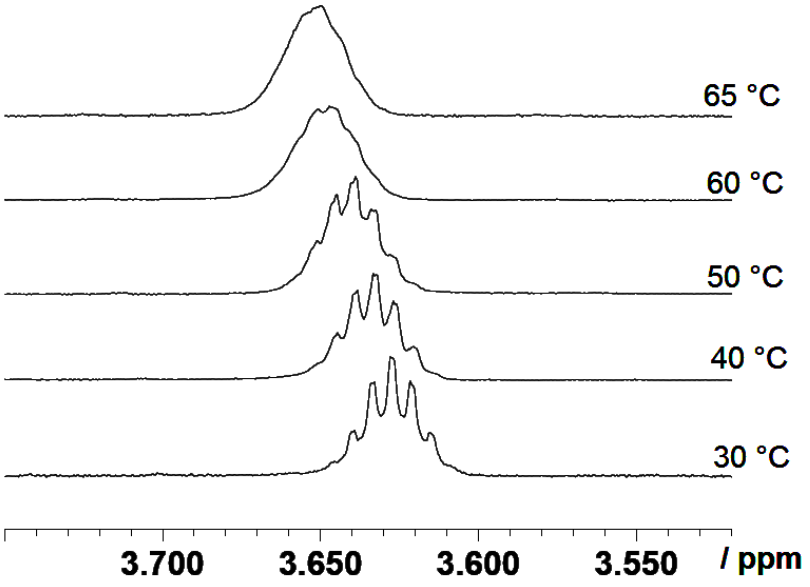

Figure S10. VT ^1H NMR spectra for a mixture of (p*R*)-**3**$^+$ and Et_3SiH in $CDCl_3$.

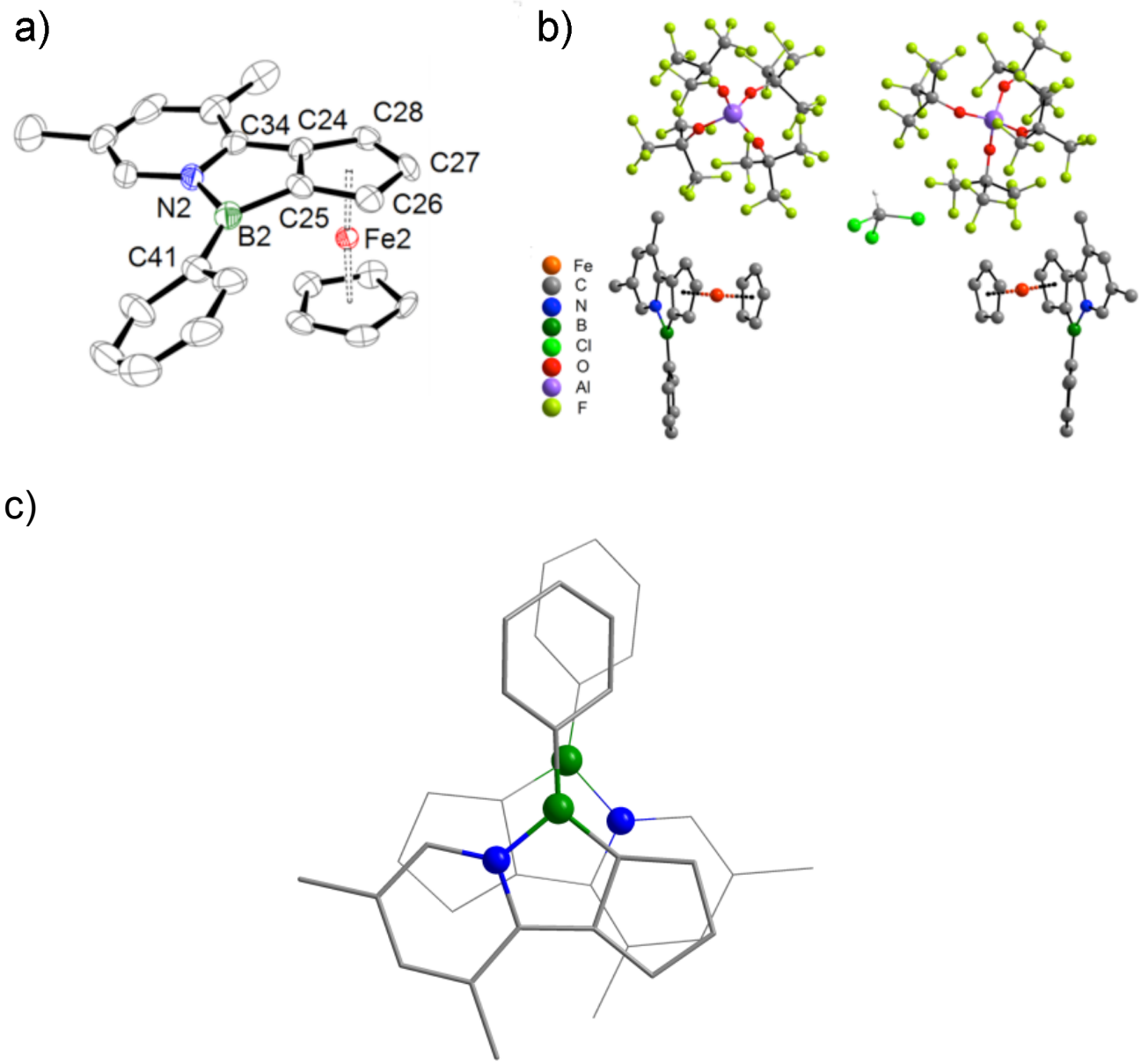

Figure S11. a) Ortep plot of the second independent molecule of (p*R*)-**3**$^+$ (50% thermal displacement ellipsoids). Hydrogen atoms and the counterion are omitted for clarity. Selected interatomic distances (Å) and angles (°): B2-N2 1.550(9), B2-C25 1.539(9), B2-C41 1.504(10), C25-B2-N2 100.6(5), C25-B2-C41 132.2(6), C41-B2-N2 127.1(6). b) Asymmetric unit of compound (p*R*)-**3**$^+$ (hydrogen atoms are omitted for clarity except in $CHCl_3$). Although the data set was acquired at 100 K, the anions were slightly disordered due to free rotation of the perfluorinated *t*-butyl groups. c) A π dimer consisting of two independent molecules of (p*R*)-**3**$^+$ (only substituted Cp rings shown).

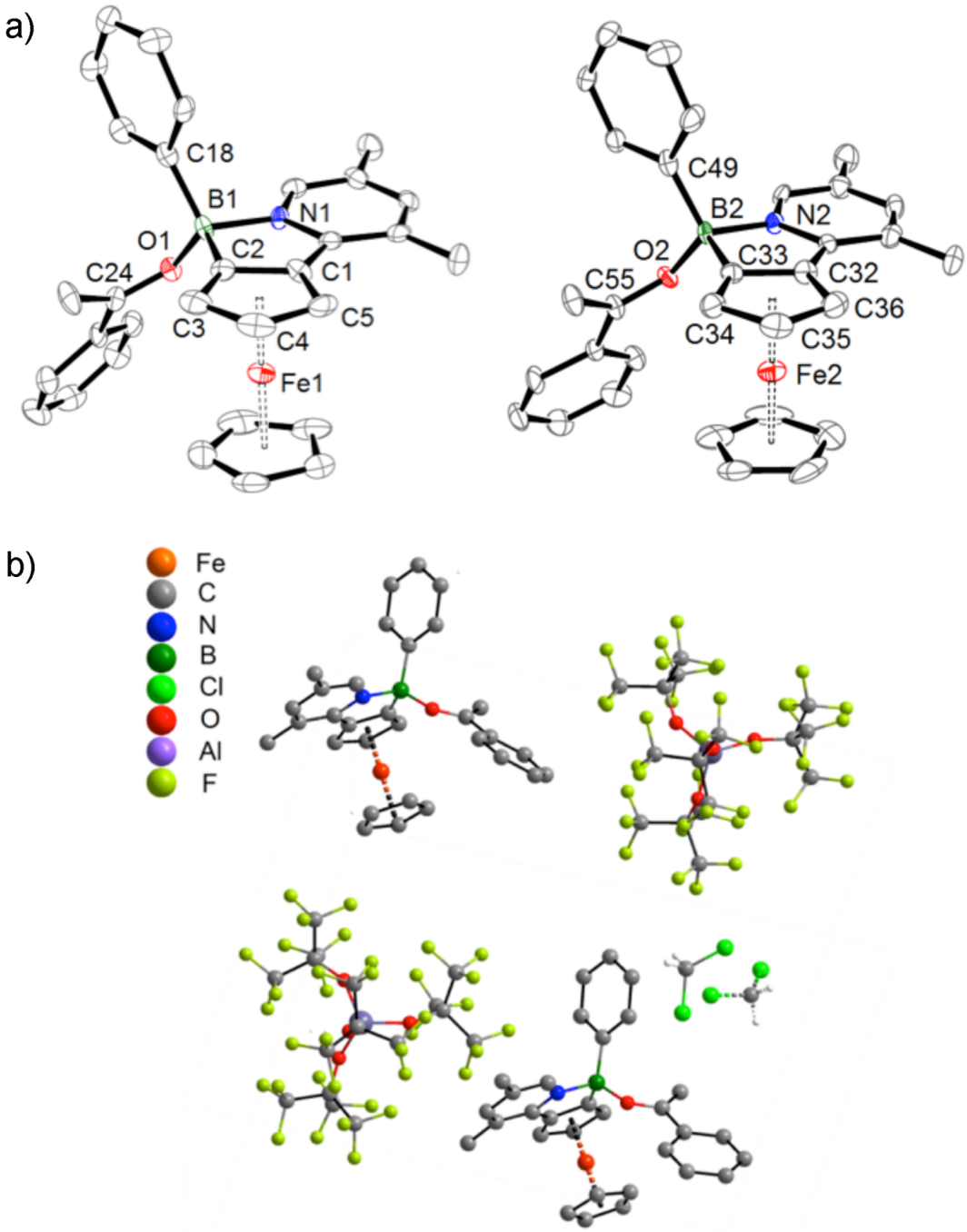

Figure S12. a) Ortep plots of two independent molecules of (p*R*)-**3**$^{+}$**(acetophenone)** (50% thermal displacement ellipsoids). Hydrogen atoms and the counterions are omitted for clarity. Selected distances (Å) [second independent molecule]: B1-N1 1.603(9) [1.592(9)], B1-O1 1.560(8) [1.577(8)], B1-C2 1.580(11) [1.593(10)], B1-C18 1.603(11) [1.594(10)], O1-C24 1.257(8) [1.255(8)]. b) Asymmetric unit of compound (p*R*)-**3**$^{+}$**(acetophenone)** (hydrogen atoms are omitted for clarity except in CH_2Cl_2). The positional disorder of the solvent CH_2Cl_2 could be modeled and refined as two parts without any problems. Both sites of the disordered CH_2Cl_2 are shown in the asymmetric cell; the site occupancy factors are 0.54 (solid) and 0.46 (dash).

Table S2. Details of X-ray analyses of (p*R*)-**3** and (p*R*)-**3**$^{+}$**(acetophenone)**

Compound	**(p*R*)-3^{+}**	**(p*R*)-3^{+} • PhC(O)Me**
CCDC	907178	907179
empirical formula	2 $[C_{23}H_{21}BFeN]^{+}$ $[C_{16}AlF_{36}O_4]^{-}\cdot CHCl_3$	2 $[C_{31}H_{29}BFeNO]^{+}$ $[C_{16}AlF_{36}O_4]^{-}\cdot CH_2Cl_2$
MW	2809.78	3015.62
T, K	100(2)	100(2)
wavelength, Å	1.54178	1.54178
crystal system	Orthorhombic	Monoclinic
space group	$P2_12_12_1$	$P2_1$
a, Å	15.9616 (6)	19.2119(3)
b, Å	20.3519 (6)	14.9703(3)
c, Å	30.5167 (8)	19.5719(3)
α, deg	90	90
β, deg	90	92.512(1)
γ, deg	90	90
V, Å^3	9913.3 (5)	5623.62(17)
Z	4	2
ρ_{calc}, g cm^{-3}	1.883	1.781
μ (Cu Kα), mm^{-1}	5.04	4.30
Crystal size, mm	0.43 × 0.28 × 0.27	0.45 x 0.32 x 0.26
θ range, deg	2.6-71.6	2.3-72.0
limiting indices	–18<=*h*<=18	–22<=*h*<=23
	–23<=*k*<=20	–15<=*k*<=17
	–36<=*l*<=35	–23<=*l*<=23
reflns collected	17455	51856
independent reflns	15330[R(int) = 0.034]	16806 [*R*(int) = 0.038]
Absorption correction	Numerical	Numerical
data/restraints/para's	15330 / 15 / 1535	16808 / 50 /1718
goodness-of-fit on F^2	1.02	1.03
final R indices	*R*1 = 0.068	*R*1 = 0.075
[I >2σ(I)] [a]	w*R*2 = 0.180	w*R*2 = 0.189
R indices (all data) [a]	*R*1 = 0.076	*R*1 = 0.088
	w*R*2 = 0.187	w*R*2 = 0.201
$Peak_{max}/hole_{min}$ (e Å^{-3})	1.37 / –0.69	1.56 / –0.66
Absolute structure parameter	0.019(5)	0.022(6)

[a] $R1 = \Sigma||F_o|-|F_c||/\Sigma|F_o|$; $wR2 = \{\Sigma[w(F_o^2-F_c^2)^2]/\Sigma[w(F_o^2)^2]\}^{1/2}$.